Monocyte-Derived Macrophages-Synovial Fibroblasts Crosstalk Unravels Oncostatin Signaling Network as a Driver of Synovitis in Osteoarthritis

Damien Laouteouet, Olivier Bortolotti, Léa Marineche, Nicole Hannemann, Manon Chambon, Yaël Glasson, Anne-Sophie Dumé, Julien de Lima, Maud Fournial, Dylan Touchet, et al.

Arthritis & Rheumatology
Vol. 0, No. 0, Month 2025, pp 1–14
DOI 10.1002/art.43299

American College of Rheumatology
Empowering Rheumatology Professionals

Monocyte-Derived Macrophages-Synovial Fibroblasts Crosstalk Unravels Oncostatin Signaling Network as a Driver of Synovitis in Osteoarthritis

Damien Laouteouet,[1] Olivier Bortolotti,[1] Léa Marineche,[1] Nicole Hannemann,[1] Manon Chambon,[1] Yaël Glasson,[2] Anne-Sophie Dumé,[2] Julien De Lima,[3] Maud Fournial,[4] Dylan Touchet,[4] Dany Séverac,[5] Felicia Leccia,[1,6] Christophe Duperray,[1,6] Henri-Alexandre Michaud,[2] Farida Djouad,[1] Benoît Le Goff,[3] Frédéric Blanchard,[3] Florence Apparailly,[1,7] and Gabriel Courties[1]

Objective. Osteoarthritis (OA) is a debilitating joint disease that is characterized by cartilage degradation, synovial inflammation, and pain. Macrophages have been implicated in OA pathology, but the origins and functions of diverse macrophage subsets seeding the synovial joint tissue remain incompletely understood. This study investigates macrophage heterogeneity, ontogeny, fate, and communication with stromal niche cells in OA.

Methods. Single-cell RNA sequencing was employed on synovial cells isolated from mice with collagenase-induced OA (CiOA) and $CD14^+$ macrophages from four patients with OA. We combined flow cytometry, genetic fate mapping, and imaging mass cytometry to profile synovial macrophage subsets. Cell–cell communication analyses were performed to investigate cellular network interactions.

Results. Three macrophage subsets with distinct gene signatures and origins were identified in CiOA, including contributions to synovial inflammation and tissue remodeling. Fate mapping via CCR2-creER and CX3CR1-creER mice revealed the expansion of monocyte-derived $TIM4^-$ $MHCII^{low/high}$ macrophages. Monocyte-independent $TIM4^+$ $CX3CR1^+$ macrophages operated a synovial niche shift, migrating near vascularized structures in the synovial subintima. Notably, the Oncostatin M (OSM)/OSM receptor (OSMR) signaling network emerged as a critical pathway linking recruited CCR2-derived macrophages to fibroblast activation. In individuals with OA, single-cell transcriptomics identified a conserved $MERTK^{low}$ $CD48^{high}$ $CCR2^+$ macrophage subpopulation as a key source of OSM.

Conclusion. Our study provides insights into macrophage subsets and their interplay with the joint microenvironment, bridging the gap between their origins, transcriptomic profiles, and roles in OA. Specifically, the OSM/OSMR axis represents a pivotal mechanism in recruited macrophage-fibroblast crosstalk, offering potential targets for novel biomarkers and therapies to manage OA-related synovitis.

Supported by the French National Research Agency (grants ANR-18-CE14-0042-01 and ANR-21-CE14-0077-01).

[1]Damien Laouteouet, PhD, Olivier Bortolotti, MSc, Léa Marineche, BSc, Nicole Hannemann, PhD, Manon Chambon, MSc, Felicia Leccia, PhD, Christophe Dupperray, PhD, Farida Djouad, PhD, Florence Apparailly, PhD, Gabriel Courties, PhD: Institute of Regenerative Medicine and Biotherapy, University of Montpellier, INSERM, Montpellier, France; [2]Yaël Glasson, MSc, Anne-Sophie Dumé, MSc, Henri-Alexandre Michaud, PharmD, PhD: Spatial Imaging Mass Cytometry and Transcriptomic facility, Montpellier Cancer Research Institute, Paris Brain Institute, University of Montpellier, INSERM, Montpellier, France; [3]Julien De Lima, MSc, Benoît Le Goff, MD, PhD, Frédéric Blanchard, PhD: Nantes Université, ONIRIS, CHU Nantes, INSERM, Regenerative Medicine and Skeleton, UMR, Nantes, France; [4]Maud Fournial, BSc, Dylan Touchet, BSc: RAM-INM, University of Montpellier, INSERM, Montpellier, France; [5]Dany Séverac, MSc: Montpellier GenomiX, University of Montpellier, CNRS, INSERM, Montpellier, France; [6]Felicia Leccia, PhD, Christophe Dupperray, PhD: Montpellier Ressources Imagerie, BioCampus, University of Montpellier, CNRS, INSERM, Montpellier, France; [7]Florence Apparailly, PhD:Clinical Department for Osteoarticular Diseases, University Hospital Lapeyronie, Montpellier, France.

Drs Laouteouet and Bortolotti are co-first authors and contributed equally to this work.

Additional supplementary information cited in this article can be found online in the Supporting Information section (http://onlinelibrary.wiley.com/doi/10.1002/art.43299).

Author disclosures and graphical abstract are available at https://onlinelibrary.wiley.com/doi/10.1002/art.43299.

Address correspondence via email to Gabriel Courties, PhD, at gabriel.courties@inserm.fr.

Submitted for publication January 6, 2025; accepted in revised form June 18, 2025.

INTRODUCTION

Osteoarthritis (OA) is the most prevalent form of degenerative joint disorder in adults, making it the leading cause of disability in the population older than 70 years.[1] With population growth and aging, the global burden of OA is projected to exceed 600 million cases of knee OA alone by 2050.[2] Despite palliative treatments for chronic pain management, surgical interventions such as joint replacement often remain the final recourse.[3] Although synovitis has been established as an important driver of OA progression, individuals with OA exhibit varying degrees of synovial inflammation.[4,5] In fact, OA exists as an heterogeneous disease with complex pathophysiology that has been stratified into disease clinical subtypes including endotypes, phenotypes, and more recently, pathotypes according to the variability in synovitis severity and other clinical features.[6–8] Hence, further investigations are currently needed to better understand OA pathogenesis and design novel targeted therapeutic interventions.

As the cellular protagonists of tissue homeostasis, inflammation, and tissue repair, macrophages from the synovial joint tissue ideally occupy a central position in OA initiation and progression. Although synovial macrophages and their secreted products are increasingly assumed to play a pivotal role in synovitis, it remains unclear which subtypes are drivers of OA pathogenesis.[9] Early attempts to identify pathogenic versus protective macrophages based on the M1/M2 classification and markers revealed rather inconclusive both in patients with OA and experimental models.[10–13] 13 In addition, macrophages depletion strategies using locally delivered clodronate-liposome or genetic mouse models resulted in contrasting outcomes in experimental OA.[14–17] Indeed, the inability to selectively target macrophage subsets, combined with the undesired effects of broad macrophage ablation, has likely hampered efforts to define their specific identities and functions in OA pathophysiology. Although joint macrophage heterogeneity has been recently characterized using single-cell RNA sequencing (scRNA-seq) in surgical mouse models of post-traumatic OA,[18] the respective contributions of locally resident and recruited macrophage subsets, as well as the cellular and molecular mechanisms underlying synovitis and OA progression, remain understudied.

In this study, we employed scRNA-seq in the collagenase-induced OA (CiOA) mouse model of OA as well as in patients with OA to investigate the origins and functional roles of macrophage subsets. By integrating flow cytometry, genetic fate mapping, and imaging mass cytometry (IMC), our findings offer novel insights into macrophage diversity, their differential contributions to OA, and their potential interactions with the synovial microenvironment.

MATERIAL AND METHODS

Animals. C57BL/6 mice were obtained from Charles River Laboratories. *Cx3cr1*-creER (B6.129P2[Cg]-*Cx3cr1*$^{tm2.1[cre/ERT2]Litt/WganJ}$, 021160), R26-tdTomato (B6.Cg Gt[ROSA]26Sor$^{tm14[CAG-tdTomato]Hze}$/J, 007914) were purchased from the Jackson Laboratory. *Ccr2*-creER mice[19] were provided by Burkhard Becher (University of Zurich) via Elodie Segura (Institut Curie). Genotyping was conducted according to the protocols provided on the Jackson Laboratory website. For fate-mapping experiments, *Ccr2-creER* and *Cx3cr1-creER* mice were crossed with R26-tdTomato reporter animals. Mice were bred and housed in our animal facility at the Institute for Neurosciences of Montpellier under specific-pathogen–free conditions. Depending on the experimental design, CiOA was induced in 10 to 12-week-old mice. All animal experiments were approved by the French Ministry of Higher Education and Research, the Languedoc-Roussillon Animal Research Ethics Committee, and the French Health Authorities, in compliance with European guidelines for animal testing.

CiOA. Mice were anesthetized with 2% isoflurane supplemented with oxygen. A small skin incision was performed on top of the patellar tendon and one unit of collagenase type VII from *Clostridium histolyticum* (Sigma-Aldrich) diluted in phosphate buffered saline (PBS) was injected (5 µl per knee joint) in the intra-articular space using a 10 µl syringe (Hamilton) with a 33-gauge needle. Two days later, a second collagenase injection was performed according to the same procedure as previously described.[20] Mice treated with PBS served as controls. OA scoring was performed on histologic assessment of the joint tissue according to a previously established semiquantitative grading system for murine models.[21]

Isolation of mouse synovial cells. Knee synovial tissues were dissected and minced into small pieces and then digested with collagenase type IV (1 mg/mL, Gibco) DNase I (0.03 mg/mL, Sigma-Aldrich) in Roswell Park Memorial Institute (RPMI-1640) medium with 10% fetal bovine Serum (FBS) for 1 hour at 37°C on a shaker at 800 revolutions per minute. The resulting cell suspension was filtered through a 35 µm nylon mesh cell strainer cap and collected in a 5 mL test tube (Corning). Cells were pelleted by centrifugation at 330 g for 5 minutes at 4°C and resuspended in PBS supplemented with 2% FBS for subsequent flow cytometry staining. All scRNA-seq raw data were deposited in the Sequence Read Archive (SRA) and are available using the bioproject accession number PRJNA1202538 (https://www.ncbi.nlm.nih.gov/sra/PRJNA1202538). Other research data are available on reasonable request.

Statistical analyses. Statistical analyses were performed using GraphPad Prism (Version 9.5.1 GraphPad Software). Data are presented as mean ± SEM. The sample size of each experiment and statistical tests used to calculate significance are reported in the figure legends. Data were first tested for normality using a D'Agostino–Pearson omnibus normality test. For the comparison of two groups, two-tailed Student's *t*-test and two-tailed Mann–Whitney tests were used for normally distributed

data and for non-normally distributed data, respectively. *P* values < 0.05 were considered to denote significance.

RESULTS

Single-cell analysis reveals macrophage subtypes transitions in CiOA synovial tissue. We employed the CiOA model in mice to investigate how OA impacts the cellular composition of synovial tissue (Figure 1A). This model closely recapitulates key pathologic features of OA observed in patients, such as synovial inflammation and cartilage degradation, irrespective of clinical variability (Figure 1B–D).[22,23] We conducted scRNA-seq on fluorescence-activated cell sorting (FACS)-sorted live synovial knee cells using the 10X Genomics platform. Uniform manifold approximation and projection (UMAP) analysis revealed 11 distinct clusters corresponding to five major cell types that were identified through differentially expressed genes (DEGs) and their enrichment for canonical markers (Figure 1E and F, Supplementary Figure 1A and B, and Supplementary Table 1). Among these, two clusters (clusters 0 and 5) were classified as synovial stromal cells because of their high expression of *Col1a1*, *Dcn*, and *Pdgfra*. Cluster 5 aligned with interstitial fibroblasts, whereas cluster 0 contained genes characteristic of both lining and sublining fibroblast subsets (Supplementary Figure 1C and Supplementary Table 2). To validate the previously reported heterogeneity of synovial fibroblasts, we mapped the expression of genes associated with lining fibroblasts (*Prg4*, *Hbegf*, *Clic5*) and sublining fibroblasts (*Thy1*, *Cd34*, *C3*).[24–26] UMAP visualization confirmed the spatial separation between lining and sublining fibroblast populations (Supplementary Figure 1D). In contrast, cluster 6 was distinguished by high expression of cartilage matrix proteins and glycoproteins, such as *Chad*, *Cilp2*, and *Comp*, identifying these cells as chondrocytes (Supplementary Figure 1C and D).[27] In addition to stromal cells, we identified granulocytes, including two neutrophil clusters (clusters 4 and 8) and an eosinophil cluster (cluster 9) characterized by gene sets such as *Csf3r*, *S100a8*, *Ly6ghematoxylin and eosin*, and *Ccr3* (Figure 1E and F, and Supplementary Figure 1B). Cluster 7 comprised two distinct subpopulations representing B cells (*Ighm*) and T cells (*Il7r*) that were marked by specific expression of *Cd19* and *Trbc2*, respectively (Figure 1E and 1F, and Supplementary Figure 1E). A further discrete cluster (cluster 10) identified endothelial cells with high expression of *Cdh5*, *Pecam1*, and *Egfl7*.

Macrophages, which prevailed in the synovial joint tissue, were characterized across three clusters (mac1, mac2, and mac3) based on co-expression of *Cd68*, *Adgre1*, and *Fcgr1* (Figure 1E–G). The mac1 cluster, which was enriched for tissue-resident macrophage (TRM) markers such as *Lyve1*, *C1qa*, *Folr2*, *Timd4*, *Vsig4*, and *Trem2*, clearly distinguished long-lived resident macrophages from the other two clusters.[28,29] In contrast, mac2 showed elevated expression of major histocompatibility complex (MHC) class II-related genes (*H2-Ab1*, *H2-Eb1*, and *Cd74*), indicating an antigen-presenting role. The mac3 cluster, which was characterized by high expression of *Spp1*, *Mmp19*, and *Arg1*, exhibited partial transcriptional overlap with mac2, particularly in shared expression of *Ccr2* and *Il1b* (Figure 1G and Supplementary Figure 1B). Pathway analysis of the top 100 DEGs in each macrophage cluster revealed distinct biologic processes (Figure 1H and Supplementary Table 3). The mac1 cluster was enriched with genes related to tissue development, wound response, vascular integrity, and complement cascades, aligning with the homeostatic role of TRMs. Mac2 was linked to hematopoietic origin, antigen presentation, and cytokine signaling pathways. Mac3, which was functionally enriched for genes related to inflammation and extracellular matrix remodeling, resembled matrisome-associated macrophages (MAM) linked to tissue fibrosis (Figure 1I),[30] a condition observed in CiOA knee joints (Figure 1J). In addition, analysis of macrophage cluster distribution across healthy and CiOA mice evidenced a strong association of mac2 and mac3 clusters with diseased joints (Figure 1K).

These findings underscore the significant impact of CiOA on the cellular landscape of synovial tissue. They particularly highlight the shifts in macrophage populations that likely drive the inflammatory and degenerative processes central to disease progression and adverse tissue remodeling.

Expanded TIM4$^-$ synovial macrophages originate from monocytes during CiOA. Corroborating scRNA-seq data, IBA1$^+$ (encoded by the *Aif1* gene) macrophages lacking Lyve-1 surface expression were found to colonize the synovial tissue of CiOA knee joints (Figure 2A and B). To explore further their monocytic origins, we employed *Ccr2$^{CreERT2/+}$:Rosa26$^{fl\text{-}tdTomato/+}$* fate-mapping mice. Flow cytometry analysis of F4/80$^+$ CD64$^+$ synovial knee joint macrophages enabled the delineation of three subpopulations based on the differential expression of MHCII and TIM4 as a surrogate tissue-resident cell surface marker. Notably, following a tamoxifen pulse, we observed a predominant tdTomato labeling in both TIM4$^-$ macrophage subsets regardless of MHCII expression. In contrast, TIM4$^+$ macrophages exhibited no detectable reporter expression, even three weeks post-induction of OA, a time point already marked by the manifestation of key disease hallmarks within the joint tissue (Figure 2C and Supplementary Figure 2). Furthermore, quantitative assessment of the synovial macrophage subsets indicated that the TIM4$^-$ subsets were primarily responsible for the substantial increase in the overall macrophage population within the knee joints affected by CiOA (Figure 2D and E). Concurrently with the influx of circulating monocytes during the first week post-CiOA,[31] local proliferation has emerged as an additional mechanism contributing to macrophage expansion within inflamed tissues.[32–36] To investigate this phenomenon, we conducted a two-hour in vivo BrdU-pulse labeling experiment during CiOA initiation (Supplementary Figure 3). During this window, ~18% of bone marrow monocytes

incorporated BrdU, in stark contrast to circulating monocytes, facilitating clear assessment of increased macrophage proliferation within CiOA knee joints by flow cytometry (Supplementary Figure 3A–C). BrdU incorporation data revealed that the proliferative activity was predominantly observed in recruited TIM4$^-$ macrophages rather than in tissue-resident TIM4$^+$ macrophages (Supplementary Figure 3D). Collectively, these findings emphasize the dual mechanisms of TIM4$^-$ macrophage expansion during CiOA, involving both the recruitment of monocytes and their subsequent proliferation.

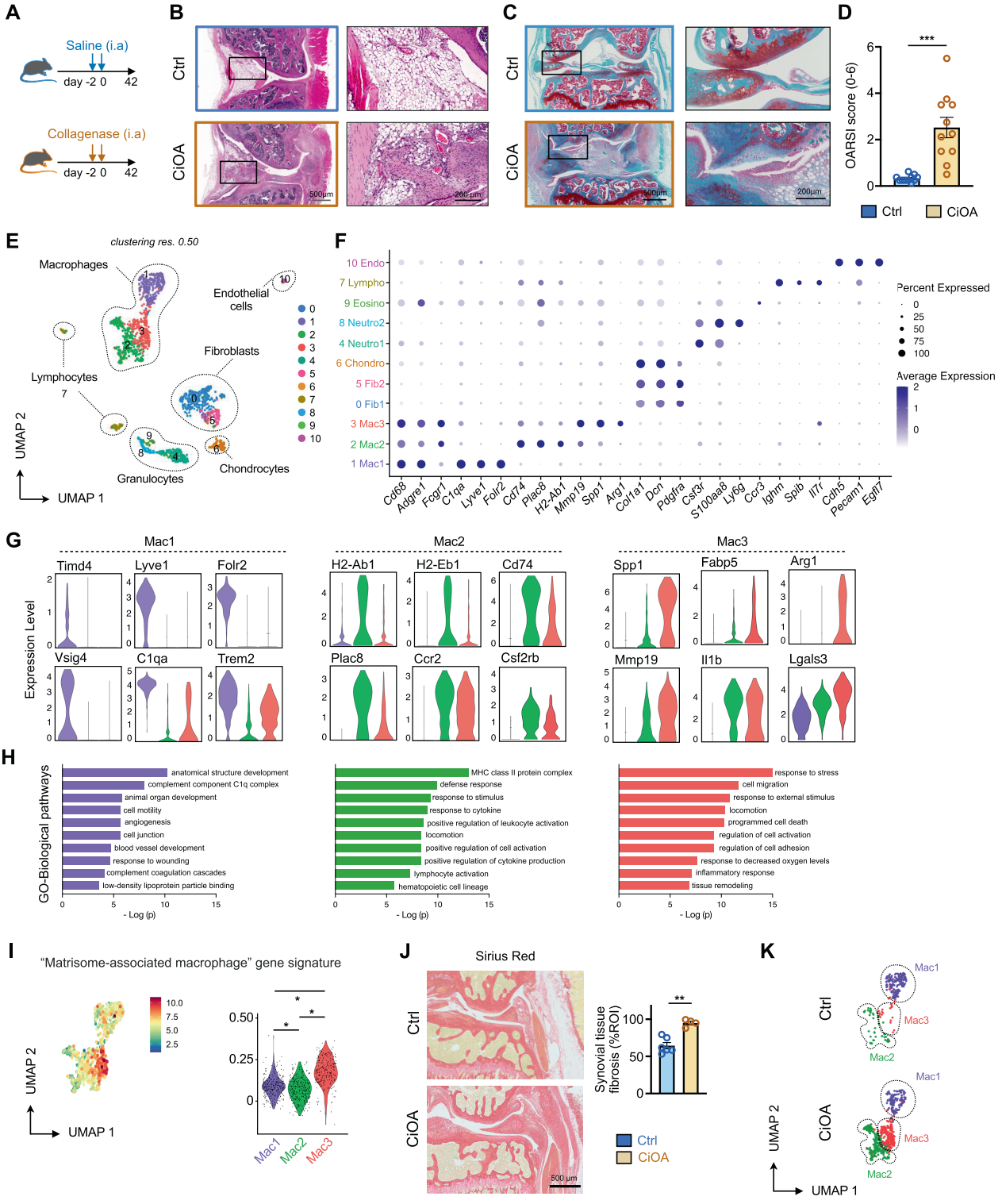

Figure 1. Legend on next page.

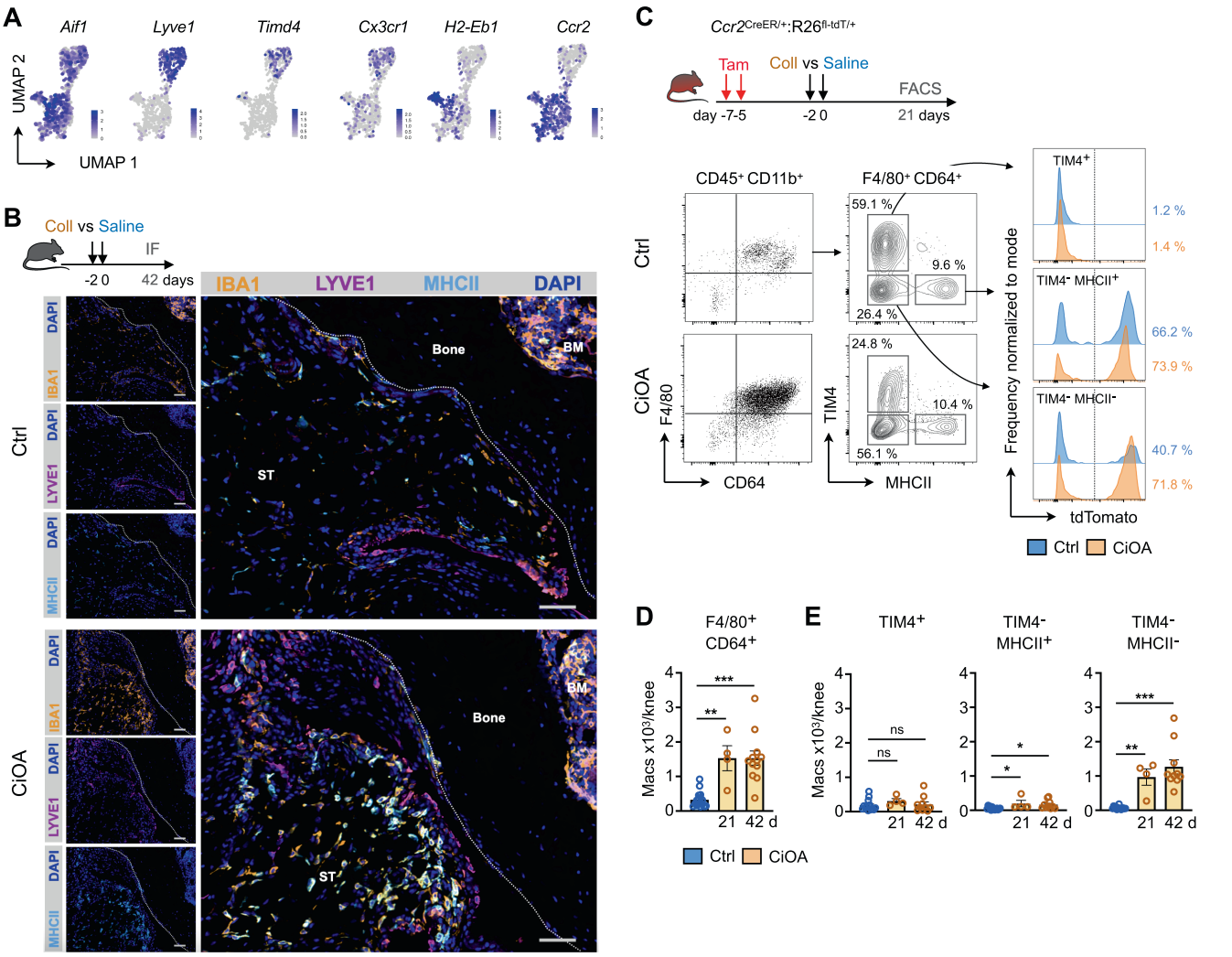

Figure 2. LYVE1$^-$ TIM4$^-$ monocyte-derived macrophages expand in CiOA joints. (A) UMAP plots showing expression of indicated marker genes related to either resident or recruited macrophages. (B) Confocal microscopy of synovial knee joints of control or mice with CiOA mice (6 weeks), showing expression of IBA1 (orange), LYVE1 (magenta), MHCII (cyan). DAPI (blue) outlines nuclei. Scale bar 50 μm. Images are representative of four mice per group. (C) CiOA was induced in Ccr2^{CreERT2}:R26-tdTomato mice after tamoxifen administration. Saline-treated mice served as control. Representative FACS plots show the percentage of macrophage subsets partitioned by TIM4 and MHCII expression among F4/80$^+$ CD64$^+$ cells across conditions. Histogram plots display the percentage of tdTomato labeling for each macrophage subset. (D) Flow cytometry quantification of synovial F4/80$^+$ CD64$^+$ macrophages from mouse knee joints with or without CiOA at indicated timepoints. (E) FACS-based enumeration of macrophage subsets (n = 4–14 per group). Data are mean ± SEM, $^*P < 0.05$, $^{**}P < 0.01$ $^{***}P < 0.001$, Kruskal-Wallis test. BM, bone marrow; CiOA, collagenase-induced osteoarthritis; Ctrl, control; FACS, fluorescence-activated cell sorting; MHC, major histocompatibility complex; ns, nonsignificant; ST, synovial tissue; UMAP, uniform manifold approximation and projection.

Figure 1. scRNA-seq reveals distinct macrophage subsets in synovial knee joint tissue during CiOA. (A) C57BL/6J mice received intra-articular collagenase VII injections and were euthanized 6 weeks later (n = 12). Control animals received saline (n = 11). (B) Representative H&E images of synovial tissues from saline- and collagenase-treated mice. Scale bar 500 μm (left) and 200 μm (right). (C) Safranin-O/Fast Green staining shows articular cartilage defects. Scale bar 500 μm (left) and 200 μm (right). (D) Bar graphs depict OARSI scores for histologic OA severity (n = 11–12/group). (E) Synovial cells were FACS-isolated and pooled for scRNA-seq. UMAP shows synovial cell clusters identified using known gene markers. (F) Dot plot showing gene expression across synovial cell clusters. (G) Violin plots of indicated gene expression levels across macrophage clusters. (H) GO pathway analysis of differentially expressed macrophage cluster genes. (I) Feature plots highlighting profibrotic MAM signature in macrophage clusters. Violin plots show the MAM score stratified by macrophage clusters. (J) Sirius Red staining shows collagen deposition in saline- and collagenase-treated joints (n = 4–6 per group). Scale bar 500 μm. (K) UMAP of annotated macrophage clusters in saline- and collagenase-treated mice. Data are mean ± SEM, $^{**}P < 0.01$, $^{***}P < 0.001$, Mann–Whitney test. Ci, collagenase-induced; Ctrl, control; GO, gene ontology; H&E, hematoxylin and eosin; FACS, fluorescence-activated cell sorting; MAM, matrisome-associated macrophage; OA, osteoarthritis; OARSI, Osteoarthritis Research Society International; MHC, major histocompatibility complex; scRNA-seq, single-cell RNA sequencing; UMAP, uniform manifold approximation and projection.

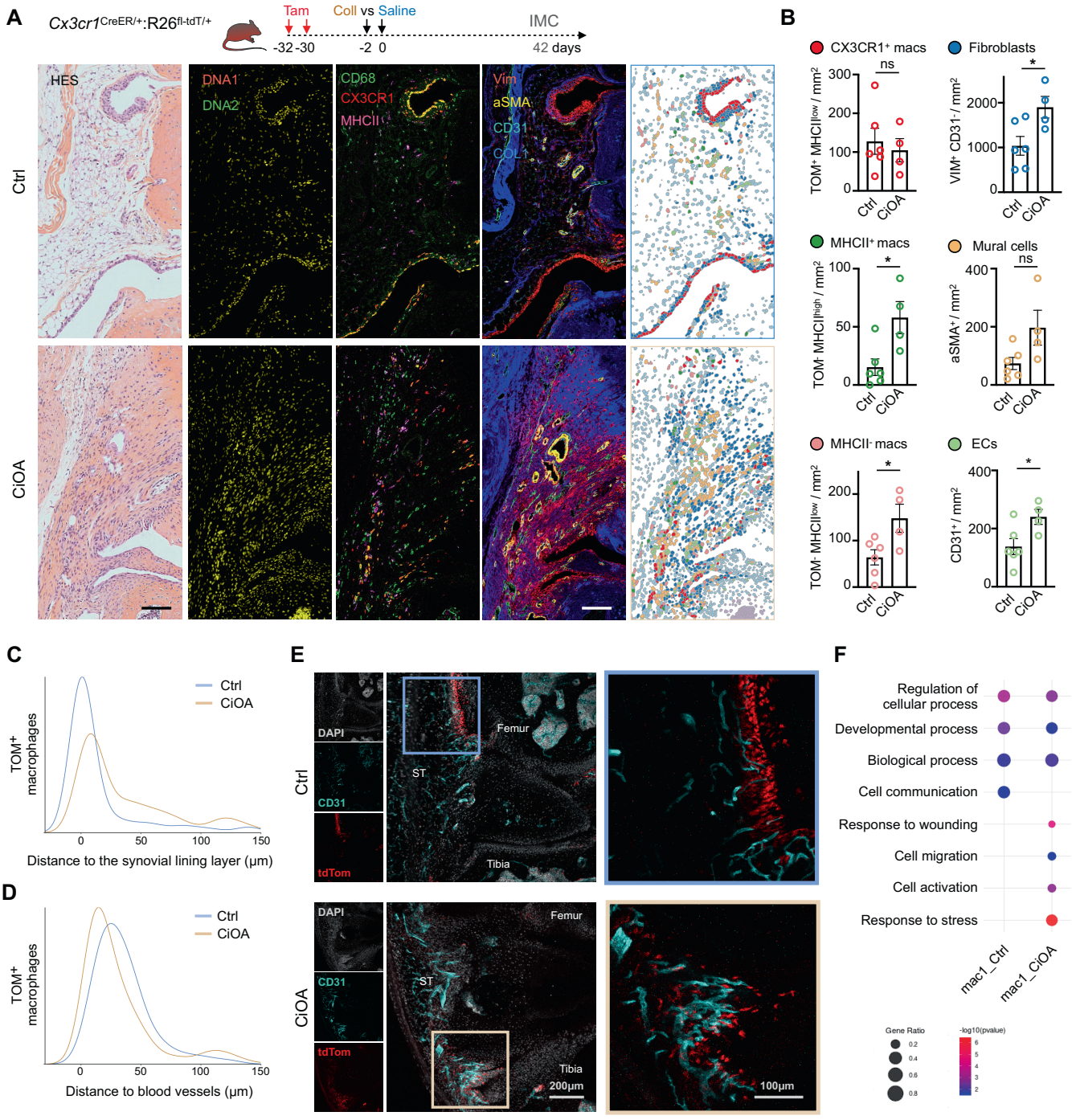

Figure 3. Tissue-resident CX3CR1$^+$ macrophages operate a niche switch in CiOA. (A) Adult Cx3cr1^{CreERT2}:R26-tdTomato mice were given tamoxifen to label resident lining macrophages. One-month post-labeling, mice underwent CiOA or saline treatment. Knee joint tissues were analyzed using IMC on day 42. Representative HES images show saline- (top) and collagenase-treated (bottom) joints. Overlaid images of CD68 (green), tdTomato (CX3CR1, red) and MHCII (magenta) highlight lining and interstitial macrophages. Vimentin (red), CD31 (cyan) and aSMA (yellow) mark fibroblasts, endothelial cells, and smooth muscle cells, respectively, while collagen I (blue) illustrate fibrotic patterns. Scale bars, 100 µm. (B) Segmentation and manual gating of IMC-generated single-cell files (.fcs) identified macrophage subsets and stromal cells. Bar graphs show IMC-based quantification of cell types (n = 4–6 per group). ns, nonsignificant, *$P < 0.05$, two-tailed Student's t-test. (C) Distance of tdTomato$^+$ macrophages from the lining layer. (D) Distance of tdTomato$^+$ macrophages from blood vessels. (E) Confocal microscopy of knee joints shows tdTomato$^+$ macrophages (red), CD31$^+$ blood vessels (cyan), and DAPI (gray) in saline-treated (top) and post-CiOA (bottom) tissues. (F) Enriched biologic processes among DEGs in the Mac1 cluster comparing CiOA with control conditions. CiOA, collagenase-induced osteoarthritis; Ctrl, control; DEG, differentially expressed gene; HES, hematoxylin-eosin-saffron; IMC, imaging mass cytometry.

CX3CR1$^+$ resident macrophages operate a spatial niche shift in synovial tissue after CiOA. Because the resident-like mac1 cluster also expressed *Cx3cr1*, we employed a tamoxifen-inducible Cx3cr1-driven lineage tracing approach to delve deeper into the fate of monocyte-independent resident macrophages after CiOA (Supplementary Figure 4).[37] After intraperitoneal tamoxifen administration in adult *Cx3cr1$^{creERT2/+}$:Rosa26$^{fl-tdTomato/+}$* mice, tdTomato labeling was irreversibly activated in CX3CR1-expressing monocytes and macrophages. Consistent with previous work, we observed a rapid decline in the frequency of CD115$^+$ tdTomato$^+$ blood monocytes, which decreased from 94.8% ± 1.2% at one-week post-tamoxifen pulse to 2.2% ± 0.1% after four weeks, which is attributable to the continual replacement of circulating monocytes derived from bone marrow hematopoietic stem and progenitor cells.[29] In contrast, CX3CR1$^+$ resident macrophages exhibited a high labeling efficiency throughout the pulse-chase experiment, although microglia demonstrated the highest percentage of tdTomato retention at four weeks (Supplementary Figure 4A and B). Subsequent flow cytometric analysis of synovial macrophages during the progression of CiOA revealed that the pool size of the tdTomato$^+$ subpopulation was largely maintained, whereas unlabeled monocyte-derived macrophages increased (Supplementary Figure 4C). The maintenance of resident macrophages alongside with increased monocyte-derived macrophages supply led us to examine their spatial distribution in the synovial niche. To this end, we developed an antibody panel for IMC to identify macrophages in relationship to structural synovial niche components (Supplementary Figure 5A–D).[38] IMC of knee joint sections from *Cx3cr1$^{CreERT2/+}$:Rosa26$^{fl-tdTomato/+}$* mice with CiOA showed a severely compromised synovial tissue microenvironment as evidenced by the loss of its well-defined architecture in healthy conditions (Figure 3A). Strikingly, the sublining interstitial region showed profound changes, resulting in a cluttered fibrotic network filled with macrophages and constituent niche cells including stromal (CD68$^-$ Vimentin$^+$), as well as mural (aSMA$^+$) and endothelial cells (CD31$^+$) forming blood vessels. In parallel to increased vascular structures and tissue fibrosis, IMC-based quantification confirmed the presence of significantly elevated recruited macrophages (CD68$^+$ tdTomato$^-$) near vascularized fibrotic regions, whereas TRMs (CD68$^+$ tdTomato$^+$) were maintained at similar levels in CiOA mice compared with controls (Figure 3B). Interestingly, tdTomato$^+$ macrophages, which initially localized in the lining niche, had shifted away and were found to cluster nearby vascularized fibrotic regions (Figure 3C–E). The mac1 cluster showed higher expression levels of genes associated with cell migration and activation, as well as responses to wounding and stress in CiOA (Figure 3F and Supplementary Table 4).

Collectively, these results underscore the dynamic nature of macrophage behavior according to their origin. They also suggest that lining CX3CR1$^+$ TRMs actively respond to stress signals from the distant interstitial sublining tissue niche.

Cell–cell interaction analysis identifies Oncostatin M–Oncostatin M receptor signaling as a major moMac-stromal communication axis in CiOA. To further examine how synovial macrophages and stromal cells differentially communicate in distinct synovial environments, we performed cell–cell communication analyses using the CellChat method.[39] Interaction plots of synovial cells across conditions suggested reinforced intercellular communication networks in mice with CiOA, particularly between macrophages and synovial stromal cells (Figure 4A and B). We next investigated information flow for signaling pathways in control and CiOA mice. When inferring significant ligand–receptor pairs (L–Rs), CellChat predicted a list of 17 putative signaling pathways exclusively active in the CiOA microenvironment (Figure 4C and Supplementary Figure 6A). The contribution of each pathway to the outgoing signaling patterns among synovial cell types identified recruited macrophages as the source of several cues, including SPP1, visfatin, and Oncostatin M (OSM). In contrast, synovial fibroblasts and chondrocytes were identified as the primary senders for periostin and midkine and EGF and CD200 signals, respectively. Overall, the intercellular signaling pathways primarily exhibited complex autocrine and paracrine communications, as each pathway targeted multiple cell types (Supplementary Figure 6A). Interestingly, this analysis predicted that OSM signals from CiOA-associated macrophages (mac2 and mac3 clusters) and neutrophils more specifically target stromal cell types. Indeed, expression patterns of the L–R pair involved in the OSM signaling network showed higher levels of *Osm* in the context of CiOA, whereas *Osmr* transcripts were exclusively found in fibroblasts and chondrocytes, identifying them as the target cells (Figure 4D and E). However, six weeks after CiOA induction, neutrophils were abundant in the bone marrow but scarce in fibrotic tissue and bone-forming osteophytes, unlike CD68$^+$ macrophages, which predominated in the damaged microenvironment. This supports the notion that monocyte-derived macrophages (mac2 and mac3 clusters) are more likely to be the primary source of OSM in CiOA synovial tissue (Supplementary Figure 6B).

OSM–OSM receptor (OSMR) axis is a potential driver of synovitis. OSM exerts broad pleiotropic effects and has implications in various processes such as proliferation, angiogenesis, tissue fibrosis, and inflammation.[40] Hence, we asked whether OSM signals are sufficient to trigger pathologic features of OA. Recombinant OSM injection into ankle joints of adult healthy wild-type mice resulted in increased numbers of synovial CD31$^+$ CD45$^-$ endothelial cells and sublining CD31$^-$ CD45$^-$ PDPN$^+$ PDGFRα$^+$ THY1$^+$ fibroblasts (Figure 5A), suggesting that OSM exerts mitogenic actions on synovial cells.[41] Although OSM was reported to contribute fibroblast chemotaxis, FACS-sorted synovial fibroblasts showed similar migration patterns regardless of OSM presence in a Boyden chamber assay (Figure 5B). In chronic joint inflammation such as rheumatoid

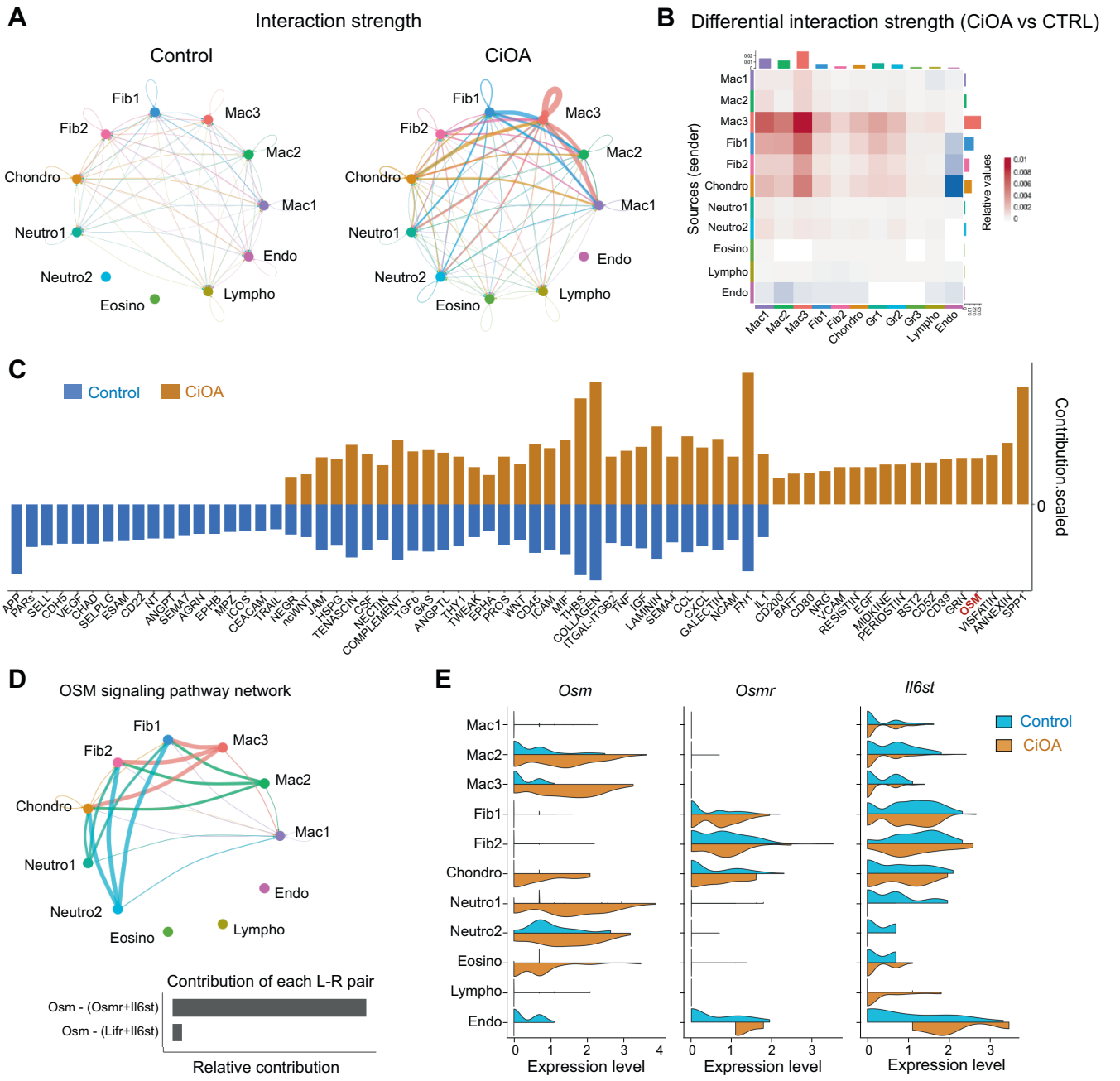

Figure 4. Cell–cell communication analyses identify immune–stromal interactions via OSM–OSMR signaling. CellChat was used for the analysis and visualization of the communications across synovial cell types and conditions. (A) Circle plots depict total interaction strength in control and in mice with CiOA. (B) Heatmap representation of the differential interaction strength between control and mice with CiOA. Red color bars indicate increased signaling in mice with CiOA compared to control animals. (C) Bar graphs show all significant signaling pathways ranked based on their differences of overall information flow within the inferred networks between control and mice with CiOA. (D) Circle plot representation of the inferred OSM signaling network and the scRNA-seq expression patterns of the OSM-(Osmr+Il6st) L–R pair in the different cell types are shown. (E) Expression distribution of *Osm* and its main receptors *Osmr* and *Il6st* in synovial knee cell types from control (blue) and mice with CiOA (orange). L–R, ligand–receptor. CiOA, collagenase-induced osteoarthritis; CTRL, control; OSM, Oncostatin M; R, receptor; scRNA-seq, single-cell RNA sequencing.

arthritis (RA), synovial fibroblasts adopt a pathogenic state marked by the expression of fibroblast activation protein (FAP) and the production of numerous cytokines, chemokines, and degrading enzymes that sustain immune cell infiltration and cartilage erosion.[24] To determine whether OSM contributes to the polarization of synovial fibroblasts toward an inflammatory, fibrotic, or destructive phenotype, we analyzed the expression of key markers of the fibroblast pathogenic switch on cultured

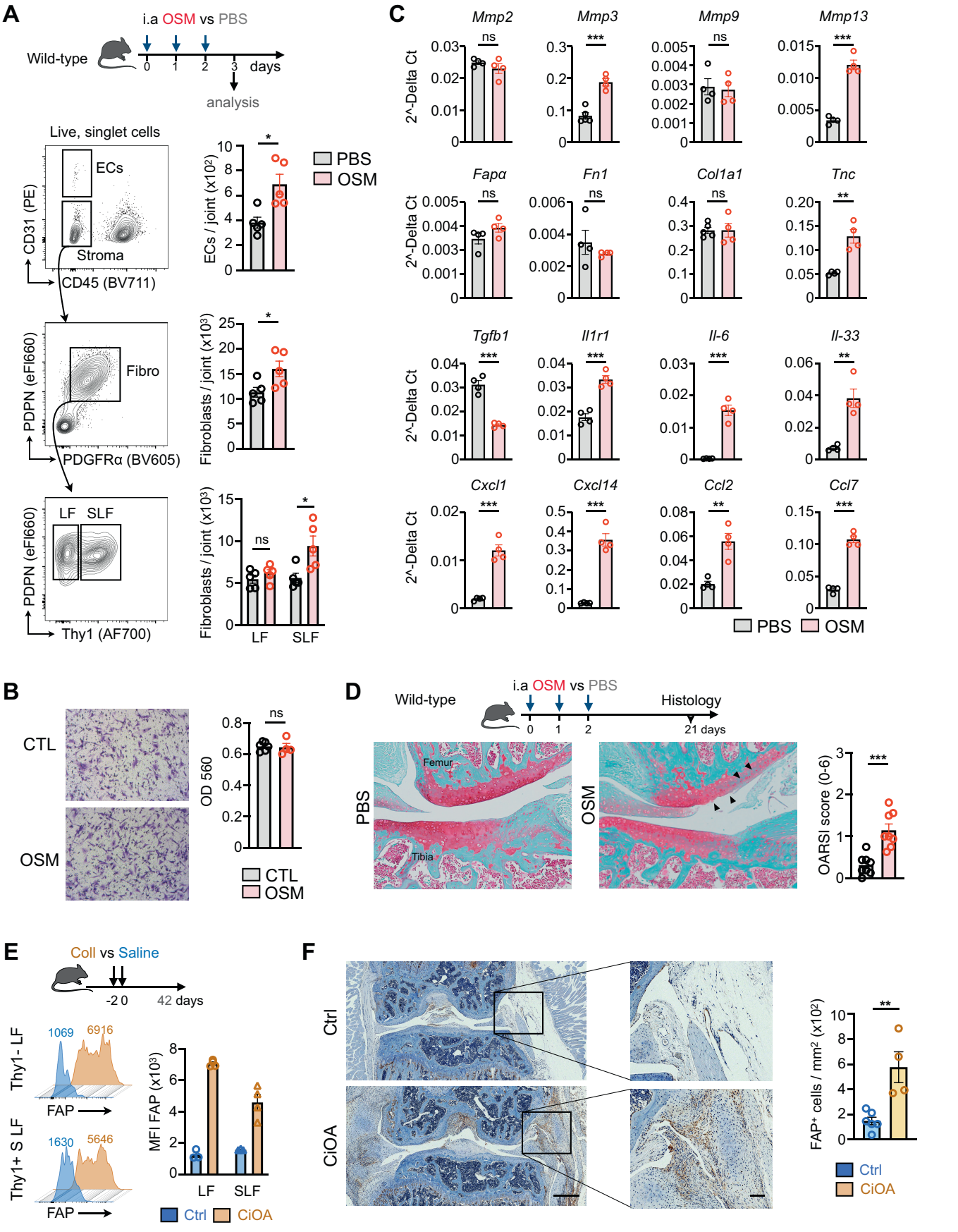

Figure 5. Legend on next page.

synovial fibroblasts incubated with or without recombinant OSM (Figure 5C). Strikingly, fibroblasts exhibited a marked pro-inflammatory signature in response to OSM stimulation as evidenced by significantly increased expression of *Ccl2*, *Ccl7*, *Cxcl1*, *Cxcl14*, *Il33*, *Il6*, and *Il1r1*. OSM had varying effects on other matrix molecules involved in fibrosis, with *Tenascin C* levels being elevated, whereas *Tgfb1* messenger RNA (mRNA) levels were significantly decreased. On the other hand, expression levels of several other extracellular matrix genes involved in tissue remodeling such as *Fibronectin 1*, *Collagen1*, or *Mmp2* and *Mmp9* remained unchanged. In contrast, *Mmp3* and *Mmp13*, two major catabolic proteases involved in cartilage degradation, were drastically up-regulated in OSM-treated synovial fibroblasts.

Consistent with gene expression profiles, three weeks after intra-articular OSM administration, histologic assessment of OSM-treated knee joints exhibited signs of cartilage defects as assessed by Safranin-O/Fast Green staining (Figure 5D), whereas collagen content was similar to contralateral saline-treated knees (data not shown). OSM signals did not significantly influence *Fap* mRNA levels in vitro, despite widespread FAP detection across fibroblast subsets and synovial tissue niches of CiOA knee joints, as demonstrated by FACS and immunohistochemistry (Figure 5E and F). These data suggest that distinct communication networks participate in synovial fibroblasts phenotypic switch and position OSM as a key factor that licenses synovial fibroblasts to produce inflammatory mediators rather than contributing to a net profibrotic phenotype.

MERTK^{low} CD48^{high} CCR2^{+} synovial macrophages drive OSM in patients with OA. To evaluate the clinical relevance of macrophage subtypes identified in experimental CiOA, we collected joint tissue from four patients with OA undergoing knee arthroplasty and isolated CD14^{+} macrophages by flow cytometry. CD14^{+} macrophages constituted the predominant immune cell population in OA synovia, accounting for 89.2% ± 3.1% of total CD45^{+} cells (Figure 6A and Supplementary Figure 7A). A total of 9057 viable single cells from these individuals were subjected to scRNA-seq using the 10X Genomics Chromium platform. At a clustering resolution of 0.15, synovial macrophages segregated into four distinct clusters (Figure 6B, Supplementary Figure 7B and Supplementary Table 5) that were annotated based on established markers.[42,43] Three of the clusters (Hu-mac1, Hu-mac2, and Hu-mac3) expressed *MERTK* and *MRC1* alongside markers associated with lining macrophages such as *TREM2*, *FOLR2*, *LYVE1*, and *TIMD4*, corresponding closely to the mac1 subset identified in mice (Figure 1). Among those, Hu-mac3 displayed a more pronounced inflammatory profile as evidenced by elevated expression of *CCL3*, *CCL4*, and *TNF* (Figure 6C and Supplementary Figure 7C). The fourth cluster, Hu-mac4, exhibited low *MERTK* and *MRC1* expression and lacked lining-associated markers (eg, TIMD4 and TREM2) but showed high expression of *CD48*, alarmins (*S100A8*, *S100A9*, *S100A12*), and inflammatory regulators like *TNFAIP3*, *NFKBIA*, and *HBEGF*. Notably, this *MERTK^{low} CD48^{high}* subset also expressed *CCR2* at notable levels. To investigate transcriptional parallels between mouse and human synovial macrophages, we mapped the DEGs from murine clusters onto the human dataset (Figure 6D). This analysis confirmed strong similarities across species, particularly for *MERTK^{low} CD48^{high}* macrophages, which in patients with OA, as in CiOA mice, expressed high levels of *NLRP3* and *IL1B* and uniquely expressed *OSM* transcripts in nearly all patients with OA (Figure 6E). Although their precise lineage requires further confirmation, the inflammatory profile of MERTK^{low} CD48^{high} macrophages, together with indirect evidence for their circulating origins,[44] suggest that OSM might also be sourced by tissue-infiltrating macrophages in human OA synovia.

DISCUSSION

The present study provides insights into the distinct origins of macrophage subtypes in the synovial tissue during steady state and osteoarthritic conditions and sheds light on their respective contribution to chronic synovitis in CiOA, a mouse model marked by a pronounced inflammatory pattern, as well as in patients with OA. Here, we highlight the OSM–OSMR axis as a promising starting point to address the interplay of monocyte-derived macrophages with synovial fibroblasts in OA, particularly for the inflammatory clinical phenotype.

Figure 5. OSM promotes a fibroinflammatory state in synovial fibroblasts. (A) Flow cytometry of endothelial cells (CD45^{-}CD31^{+}), lining (CD45^{-}CD31^{-}PDPN^{+}PDGFRα^{+}Thy1^{-}), and sublining fibroblasts (CD45^{-}CD31^{-}PDPN^{+}PDGFRα^{+}Thy1^{+}) after intra-articular injections of rOSM in C57BL/6 mice (n = 5). Contralateral joints received PBS as controls. (B) Migration assay using Boyden chambers with synovial fibroblasts seeded in the upper chamber. Migrated cells were stained and measured at 560 nm after 24 hours of migration toward rOSM or PBS in the lower chamber (n = 4–5 per group). (C) RT–qPCR of selected markers in FACS-sorted fibroblasts (PDPN^{+}PDGFRα^{+}) incubated with rOSM in vitro (n = 4–5 mice per group). (D) Safranin-O/Fast Green-stained sections highlight proteoglycan loss and cartilage fibrillation in C57BL/6 mice (n = 8) three weeks after intra-articular injections of rOSM (right knee) or PBS (left knee). Bar graph shows cartilage damage scores. (E) Flow cytometry of FAP expression in Thy1^{-} lining and Thy1^{+} sublining fibroblasts in control and CiOA mice. Bar graphs show geometric mean FAPα signal. (F) FAPα immunostaining in synovial tissues of control and CiOA. Scale bar 500 μm for left panels and 100 μm for enlarged images. Bar graphs show QuPath quantification of FAPα^{+} cells (n = 4–6 mice per group). Mann–Whitney test; ns, not significant; *P < 0.05; **P < 0.01, and ***P < 0.001. CiOA, collagenase-induced osteoarthritis; CTL, control; Ctrl; control; EC, endothelial cell; FACS, fluorescence-activated cell sorting; FAP, fibroblast activation protein; LF, lining fibroblast; MFI, mean fluorescence intensity; ns, nonsignificant; OARSI, Osteoarthritis Research Society International; OD, optical density; OSM, Oncostatin M; PBS, phosphate buffered saline; r, recombinant; RT–qPCR, quantitative reverse transcription PCR; SLF, sublining fibroblast.

Consistent with recent synovial scRNA-seq studies in mice simulating OA caused after a traumatic injury, our findings confirm that the healthy knee synovial tissue harbors a predominant macrophage subset characterized by residency genes (*Trem2*, *Cx3cr1*, *Vsig4*) but also share conserved features reminiscent to TRMs seeding various other organs body such as the expression

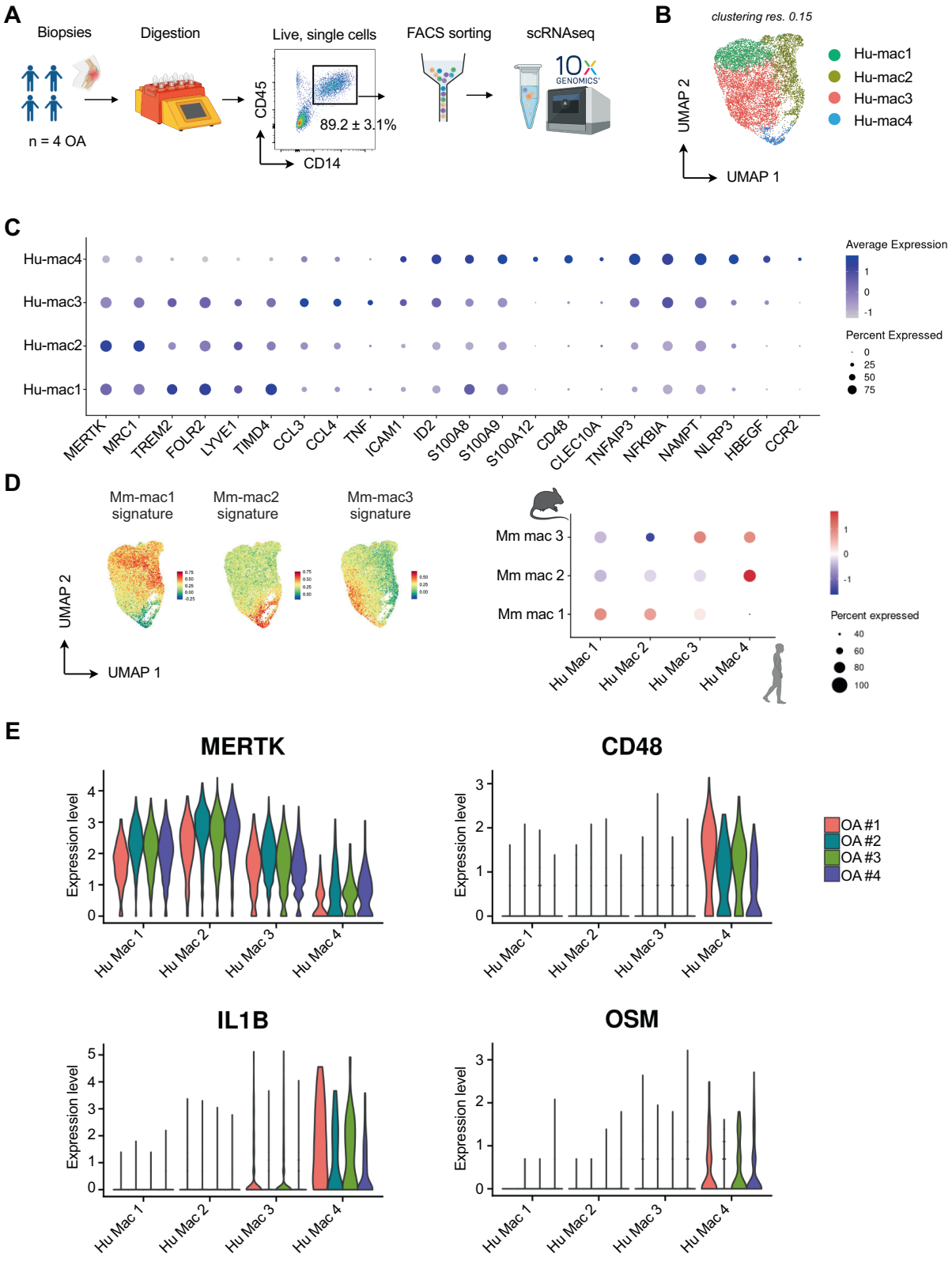

Figure 6. Legend on next page.

of *Timd4*, *Lyve1*, and *Folr2*.[18,28,29] In line with previous observations, we also corroborate the distinct synovial tissue positioning of CX3CR1^{+} macrophages and MHCII^{+} macrophages in healthy lining and interstitial synovial niche microenvironments, respectively.[37,45] Although the precise fetal origin of synovial macrophage subsets and how they establish in the developing joint have yet to be formally assessed, our findings in *Cx3cr1*^{CreER}-Rosa^{tdTomato} mice support the long-lived nature of lining TRM. Despite their efferocytic and anti-inflammatory actions at steady state, the role of macrophages seeding the lining layer during joint inflammation remains puzzling. Their depletion before joint inflammation resulted in contrasting disease outcomes in OA, and their protective role in mouse models of RA has been challenged by their more recently described activation status promoting innate immune cell supply.[37,46] This apparent contradiction might arise from either broad or macrophage subset-specific depletion that activate surrounding synovial niche cells, thereby triggering spontaneous joint inflammation.[47] By combining Cx3cr1-based fate mapping and IMC, we demonstrate that the size of the lining macrophage pool remains unchanged in mice with OA but undergoes spatial reorganization toward the interstitial fibrotic areas of the synovial tissue. Accumulation of CX3CR1^{+} macrophages near poorly structured blood vessels was associated with a gene signature indicative of inflammatory response and migration pathways. However, a limitation of our study lies in the challenge of recovering sufficient endothelial cells to identify potential signaling networks that would provide insight into mechanisms driving this niche shift. Hence, future studies are necessary to assess whether lining TRM restrain or promote pathologic angiogenesis in OA.

Using *Ccr2*-based fate-mapping strategy, regardless of MHCII expression, TIM4^{-} synovial macrophage subtypes, which highly expressed Ccr2, achieved efficient tdTomato labeling upon tamoxifen administration in *Ccr2*^{CreER}-Rosa^{tdTomato} mice, indicating their monocytic origin. Although recent trajectory inference analyses have suggested resident macrophages may also give rise to activated phenotypes, including those expressing CCR2 and SPP1, our direct fate-mapping data strongly supports that the significant numerical expansion driving synovitis in this model originates primarily from the recruitment and proliferation of CCR2-dependent, TIM4^{-} monocytes.[48] Further experimental lineage tracing studies will be valuable to definitively reconcile the relative contributions of resident macrophage diversification versus monocyte recruitment to the full spectrum of macrophage phenotypes in different OA models. In CiOA, increased vascularization and fibrosis were associated with interstitial tissue colonization by recruited monocyte-derived macrophages, indicating their role in driving synovitis. During CiOA, paralleling increased vascularization and fibrosis, and the interstitial tissue niche was profoundly affected by colonization of recruited monocyte-derived macrophages displaying a mixed profibrotic and pro-inflammatory gene signature. Their mixed pro-inflammatory and profibrotic transcriptomic profile is reminiscent to those of MAM identified in multiple fibrosing disorders including patients with OA, suggesting a role in driving synovitis and adverse tissue remodeling.[30]

Understanding intercellular communication networks in relation to synovial cell diversity is essential for uncovering how OA disrupts joint health and function. Here, we highlight the OSM–OSMR axis as a key mediator of the interplay between monocyte-derived macrophages and synovial fibroblasts in mice with CiOA. Importantly, our findings underscore the existence of an analogous MERTK^{low} CD48^{high} CCR2^{+} population to *Osm* expressing murine macrophages in human osteoarthritic synovial tissues. Development of strategies for in vivo OSM specific targeting in recruited macrophage subsets will provide a better understanding of the mechanisms by which OSM influence the stromal microenvironment. Although OSM levels are elevated in a subset of patients with OA, whether the OSM/OSMR circuit also associates with a clinical inflammatory phenotype warrant further investigations.[49] Defining synovial cell composition and identifying specific molecular networks to knee OA subtypes, as outlined by current stratification systems, may represent a critical step toward targeted therapeutic interventions for patients.

ACKNOWLEDGMENTS

The authors thank the functional exploration platform Réseau des Animaleries de Montpellier RAM-Neuro for their assistance with animal husbandry, breeding, and maintenance throughout this study. We acknowledge the Réseau d'Histologie Expérimentale de Montpellier facility supported by SIRIC (Sites de Recherche Intégrée sur le Cancer) Montpellier Cancer (Grant INCa_Inserm_DGOS_12553), the European regional development foundation and the Occitania region (FEDER-FSE 2014–2020 Languedoc-Roussillon) for processing our animal tissues, histology technics and expertise. We also thank the Montpellier Ressources Imagerie flow cytometry core for assistance with cell sorting, and the Montpellier GenomiX (MGX) Platform of Montpellier for single-cell library preparations and sequencing. MGX acknowledges financial support from France Génomique National infrastructure, funded as part of

Figure 6. MERTK^{low} CD48^{high} synovial macrophages drive OSM expression in patients with OA. (A) Schematic overview of the experimental workflow. Synovial biopsies from four patients with OA were digested to obtain single cells, followed by CD14^{+} macrophage isolation via FACS sorting and scRNA-seq analysis using the 10X Genomics platform. (B) UMAP plot showing four clusters of CD14^{+} synovial macrophages from patients with OA, with cell identities assigned based on established gene expression markers. (C) Dot plot illustrating the expression levels of selected genes across the identified macrophage clusters. Dot size represents the percentage of cells expressing the gene, and color intensity indicates average expression. (D) DEGs of murine macrophage clusters were used to score macrophages in synovial macrophage clusters from patients with OA. (E) Violin plots showing the expression of representative genes (MERTK, CD48, IL1B, and OSM) across macrophage clusters, stratified by individual patients with OA. DEG, differentially expressed gene; FACS, fluorescence-activated cell sorting; IL, interleukin; OA, osteoarthritis; OSM, Oncostatin M; scRNA-seq, single-cell RNA sequencing; UMAP, uniform manifold approximation and projection.

"Investissement d'Avenir" program managed by Agence Nationale pour la Recherche (contract ANR-10-INBS-09). We thank Dr. Salwa Sebti for proofreading the manuscript. We acknowledge BioRender (https://BioRender.com/v82d643) for cartoon components.

AUTHOR CONTRIBUTIONS

All authors contributed to at least one of the following manuscript preparation roles: conceptualization AND/OR methodology, software, investigation, formal analysis, data curation, visualization, and validation AND drafting or reviewing/editing the final draft. As corresponding author, Dr Courties confirms that all authors have provided the final approval of the version to be published and takes responsibility for the affirmations regarding article submission (eg, not under consideration by another journal), the integrity of the data presented, and the statements regarding compliance with institutional review board/Declaration of Helsinki requirements.

REFERENCES

1. Hunter DJ, Bierma-Zeinstra S. Osteoarthritis. Lancet 2019;393(10182):1745–1759.
2. Steinmetz JD, Culbreth GT, Haile LM, et al; GBD 2021 Osteoarthritis Collaborators. Global, regional, and national burden of osteoarthritis, 1990–2020 and projections to 2050: a systematic analysis for the Global Burden of Disease Study 2021. Lancet Rheumatol 2023;5(9):e508–e522.
3. Kolasinski SL, Neogi T, Hochberg MC, et al. 2019 American College of Rheumatology/Arthritis Foundation guideline for the management of osteoarthritis of the hand, hip, and knee. Arthritis Rheumatol 2020;72(2):220–233.
4. Perry TA, Parkes MJ, Hodgson RJ, et al. Association between bone marrow lesions & synovitis and symptoms in symptomatic knee osteoarthritis. Osteoarthritis Cartilage 2020;28(3):316–323.
5. Wyatt LA, Nwosu LN, Wilson D, et al. Molecular expression patterns in the synovium and their association with advanced symptomatic knee osteoarthritis. Osteoarthritis Cartilage 2019;27(4):667–675.
6. Angelini F, Widera P, Mobasheri A, et al. Osteoarthritis endotype discovery via clustering of biochemical marker data. Ann Rheum Dis 2022;81(5):666–675.
7. Dell'Isola A, Allan R, Smith SL, et al. Identification of clinical phenotypes in knee osteoarthritis: a systematic review of the literature. BMC Musculoskelet Disord 2016;17(1):425.
8. Boutet M-A, Nerviani A, Fossati-Jimack L, et al. Comparative analysis of late-stage rheumatoid arthritis and osteoarthritis reveals shared histopathological features. Osteoarthritis Cartilage 2024;32(2):166–176.
9. Thomson A, Hilkens CMU. Synovial macrophages in osteoarthritis: the key to understanding pathogenesis? Front Immunol 2021;12:678757.
10. Caron JP, Fernandes JC, Martel-Pelletier J, et al. Chondroprotective effect of intraarticular injections of interleukin-1 receptor antagonist in experimental osteoarthritis. Suppression of collagenase-1 expression. Arthritis Rheum 1996;39(9):1535–1544.
11. Kraus VB, McDaniel G, Huebner JL, et al. Direct in vivo evidence of activated macrophages in human osteoarthritis. Osteoarthritis Cartilage 2016;24(9):1613–1621.
12. Liu B, Zhang M, Zhao J, et al. Imbalance of M1/M2 macrophages is linked to severity level of knee osteoarthritis. Exp Ther Med 2018;16(6):5009–5014.
13. Zhang H, Lin C, Zeng C, et al. Synovial macrophage M1 polarisation exacerbates experimental osteoarthritis partially through R-spondin-2. Ann Rheum Dis 2018;77(10):1524–1534.
14. van Lent PLEM, Blom AB, van der Kraan P, et al. Crucial role of synovial lining macrophages in the promotion of transforming growth factor β-mediated osteophyte formation. Arthritis Rheum 2004;50(1):103–111.
15. Blom AB, van Lent PLEM, Holthuysen AEM, et al. Synovial lining macrophages mediate osteophyte formation during experimental osteoarthritis. Osteoarthritis Cartilage 2004;12(8):627–635.
16. Bailey KN, Furman BD, Zeitlin J, et al. Intra-articular depletion of macrophages increases acute synovitis and alters macrophage polarity in the injured mouse knee. Osteoarthritis Cartilage 2020;28(5):626–638.
17. Wu CL, McNeill J, Goon K, et al. Conditional macrophage depletion increases inflammation and does not inhibit the development of osteoarthritis in obese macrophage fas-induced apoptosis-transgenic mice. Arthritis Rheumatol 2017;69(9):1772–1783.
18. Sebastian A, Hum NR, McCool JL, et al. Single-cell RNA-seq reveals changes in immune landscape in post-traumatic osteoarthritis. Front Immunol 2022;13:938075.
19. Croxford AL, Lanzinger M, Hartmann FJ, et al. The cytokine GM-CSF drives the inflammatory signature of CCR2+ monocytes and licenses autoimmunity. Immunity 2015;43(3):502–514.
20. Maumus M, Noël D, Ea HK, et al. Identification of TGFβ signatures in six murine models mimicking different osteoarthritis clinical phenotypes. Osteoarthritis Cartilage 2020;28(10):1373–1384.
21. Glasson SS, Chambers MG, Van Den Berg WB, et al. The OARSI histopathology initiative - recommendations for histological assessments of osteoarthritis in the mouse. Osteoarthritis Cartilage 2010;18(suppl 3):S17–S23.
22. van der Kraan PM, Vitters EL, van Beuningen HM, et al. Degenerative knee joint lesions in mice after a single intra-articular collagenase injection. A new model of osteoarthritis. J Exp Pathol (Oxford). 1990;71(1):19–31.
23. Bapat S, Hubbard D, Munjal A, et al. Pros and cons of mouse models for studying osteoarthritis. Clin Transl Med 2018;7(1):36.
24. Croft AP, Campos J, Jansen K, et al. Distinct fibroblast subsets drive inflammation and damage in arthritis. Nature 2019;570(7760):246–251.
25. Stephenson W, Donlin LT, Butler A, et al. Single-cell RNA-seq of rheumatoid arthritis synovial tissue using low-cost microfluidic instrumentation. Nat Commun 2018;9(1):791.
26. Friščić J, Böttcher M, Reinwald C, et al. The complement system drives local inflammatory tissue priming by metabolic reprogramming of synovial fibroblasts. Immunity 2021;54(5):1002–1021.e10.
27. Sebastian A, McCool JL, Hum NR, et al. Single-cell RNA-seq reveals transcriptomic heterogeneity and post-traumatic osteoarthritis-associated early molecular changes in mouse articular chondrocytes. Cells 2021;10(6):1462.
28. Chakarov S, Lim HY, Tan L, et al. Two distinct interstitial macrophage populations coexist across tissues in specific subtissular niches. Science 2019;363(6432):eaau0964.
29. Dick SA, Wong A, Hamidzada H, et al. Three tissue-resident macrophage subsets coexist across organs with conserved origins and life cycles. Sci Immunol 2022;7(67):eabf7777.
30. Ouyang JF, Mishra K, Xie Y, et al. Systems level identification of a matrisome-associated macrophage polarisation state in multi-organ fibrosis. eLife 2023;12:e85530.
31. Cremers NAJ, van den Bosch MHJ, van Dalen S, et al. S100A8/A9 increases the mobilization of pro-inflammatory Ly6C^{high} monocytes to the synovium during experimental osteoarthritis. Arthritis Res Ther 2017;19(1):217.
32. Jenkins SJ, Ruckerl D, Cook PC, et al. Local macrophage proliferation, rather than recruitment from the blood, is a signature of T_H2 inflammation. Science 2011;332(6035):1284–1288.

33. Robbins CS, Hilgendorf I, Weber GF, et al. Local proliferation dominates lesional macrophage accumulation in atherosclerosis. Nat Med 2013;19(9):1166–1172.
34. Davies LC, Rosas M, Jenkins SJ, et al. Distinct bone marrow-derived and tissue-resident macrophage lineages proliferate at key stages during inflammation. Nat Commun 2013;4(1):1886.
35. Epelman S, Lavine KJ, Beaudin AE, et al. Embryonic and adult-derived resident cardiac macrophages are maintained through distinct mechanisms at steady state and during inflammation. Immunity 2014;40(1):91–104.
36. Vanneste D, Bai Q, Hasan S, et al. MafB-restricted local monocyte proliferation precedes lung interstitial macrophage differentiation. Nat Immunol 2023;24(5):827–840.
37. Culemann S, Grüneboom A, Nicolás-Ávila JÁ, et al. Locally renewing resident synovial macrophages provide a protective barrier for the joint. Nature 2019;572(7771):670–675.
38. Giesen C, Wang HAO, Schapiro D, et al. Highly multiplexed imaging of tumor tissues with subcellular resolution by mass cytometry. Nat Methods 2014;11(4):417–422.
39. Jin S, Guerrero-Juarez CF, Zhang L, et al. Inference and analysis of cell-cell communication using CellChat. Nat Commun 2021;12(1):1088.
40. West NR, Owens BMJ, Hegazy AN. The Oncostatin M-stromal cell axis in health and disease. Scand J Immunol 2018;88(3):e12694.
41. Fearon U, Mullan R, Markham T, et al. Oncostatin M induces angiogenesis and cartilage degradation in rheumatoid arthritis synovial tissue and human cartilage cocultures. Arthritis Rheum 2006;54(10):3152–3162.
42. Kuo D, Ding J, Cohn IS, et al. HBEGF^{+} macrophages in rheumatoid arthritis induce fibroblast invasiveness. Sci Transl Med 2019;11(491):eaau8587.
43. Alivernini S, MacDonald L, Elmesmari A, et al. Distinct synovial tissue macrophage subsets regulate inflammation and remission in rheumatoid arthritis. Nat Med 2020;26(8):1295–1306.
44. Kurowska-Stolarska M, Alivernini S. Synovial tissue macrophages in joint homeostasis, rheumatoid arthritis and disease remission. Nat Rev Rheumatol 2022;18(7):384–397.
45. Misharin AV, Cuda CM, Saber R, et al. Nonclassical Ly6C(-) monocytes drive the development of inflammatory arthritis in mice. Cell Rep 2014;9(2):591–604.
46. Zec K, Schonfeldova B, Ai Z, et al. Macrophages in the synovial lining niche initiate neutrophil recruitment and articular inflammation. J Exp Med 2023;220(8):e20220595.
47. Mass E, Nimmerjahn F, Kierdorf K, et al. Tissue-specific macrophages: how they develop and choreograph tissue biology. Nat Rev Immunol 2023;23(9):563–579.
48. Knights AJ, Farrell EC, Ellis OM, et al. Synovial macrophage diversity and activation of M-CSF signaling in post-traumatic osteoarthritis. eLife 2025;12:RP93283.
49. Iijima H, Zhang F, Ambrosio F, et al. Network-based cytokine inference implicates Oncostatin M as a driver of an inflammation phenotype in knee osteoarthritis. Aging Cell 2024;23(2):e14043.